Self-Calibrated Ion-Selective Electrodes

Nafesa Adil, Renjie Wang†, Xuewei Wang*

Department of Chemistry, Virginia Commonwealth University, 1001 W. Main Street, Richmond, VA 23284.

ABSTRACT: Ion-selective electrode (ISE) potentiometry is reliable only if on-site calibration using a standard solution is performed before the ion measurement. The complex device and operation required for calibration hinder the implementation of ISEs in decentralized sensing. Reported herein is a new type of ISE that is calibrated by a built-in component of the sensor without requiring any fluid handling processes. The indicator and reference electrodes are connected by a thin ionic conductor such as an aqueous phase containing the measuring ions in a capillary tube. This connection establishes a baseline electromotive force (EMF) that incorporates phase boundary potentials across multiple interfaces of the electrochemical cell and serves as a one-point calibration. Unlike conventional ISEs relying on absolute EMF readings, the proposed sensor utilizes a sample-induced EMF change relative to the baseline for ion measurements. The variability in relative EMF is found to be < 2.0 mV for multiple full potentiometric sensors consisting of plasticizer-based K^+ ISEs and hydrogel-based Ag/AgCl reference electrodes. This value is significantly smaller than the variability of absolute EMF readouts in similar sensors without the self-calibration design. Moreover, when the ion-conducting calibration bridge has a low concentration of primary ions, low ion mobility, and/or a small contact area with the indicator and reference phases, it does not compromise the Nernstian response slope toward the analyte ions in the sample and therefore does not need to be removed for sample testing. The accuracy of single-use self-calibrated K^+ sensors in testing undiluted human blood samples is validated using a commercial blood gas analyzer as the reference method. This fluidics-free self-calibration strategy opens up new opportunities for ion sensing in disposable, wearable, and implantable devices.

INTRODUCTION

Ionophore-based ISEs offer exceptional selectivity, high logarithmic linearity, rapid response time, and excellent reversibility, making them ideal for measuring electrolyte activities in biofluids such as blood, plasma, and urine. They have achieved tremendous commercial success in fully automated blood gas/electrolyte analyzers and clinical chemistry analyzers used by healthcare professionals. In recent years, there has been a growing interest in affordable and accessible electrolyte measurements in decentralized locations. For instance, the development of home-use electrolyte sensors capable of frequent testing of K^+, Ca^{2+}, and Na^+ in capillary blood holds the potential to revolutionize the self-management of chronic renal, heart, parathyroid, and hypothalamus disorders.[1-4] Epidermal, transdermal, and implanted electrolyte sensors for sweat and interstitial fluids may permit real-time monitoring of electrolyte homeostasis to guide timely interventions.[5-10] Since the composition and fabrication of ISEs have been well established for decades, it might seem that ISEs can be rapidly integrated into wearable, implantable, and at-home sensing devices once appropriate engineering is applied. However, despite significant engineering advancements,[5-10] the use of ISEs as accurate ion monitors in decentralized settings has not been successful to the best of our knowledge.

One major hurdle in utilizing ISEs for decentralized ion monitoring is the need for on-site calibration. In commercial handheld, benchtop, and laboratory electrolyte analyzers, each ISE is calibrated using standard solutions with known analyte activities before and/or between measurements. This calibration process involves complex instruments comprising standard solutions, fluidic channels, and fluid control modules such as pumps, actuators, and valves. Batch calibration and factory calibration are possible approaches to eliminating the mandatory individual calibration at the point of use. The prerequisite for batch calibration is that all ISEs fabricated in the same large batch have the nearly same calibration curves (the standard potential, E°, and the response slope). Electrolyte measurements for medical diagnostics often require an EMF error of no more than 1-2 mV. However, such a small variation is extremely challenging to obtain in an EMF range spanning hundreds of mV. The EMF measurement is susceptible to subtle variations at any interfaces of the electrochemical cell involving the metal or carbon electrode, the ion-to-electron transducer, the sensing membrane, and the reference electrode components.[11,12] The prerequisite for individual factory calibration is that the electrodes do not undergo any changes during storage. Data on the storage stability of ISEs is very limited, but aging of any components, interpenetration between adjacent phases, and exposure to ambient gases, moisture, and light can lead to unpredictable EMF drifts.[13,14] The groups of Bakker, Bobacka, and Yoshida explored coulometry and constant potential coulometry as alternative readout modes of ion-selective membranes with motivations including eliminating the calibration process.[15-19] However, the authors noted limitations such as fluid handling requirements and systematic errors, and the coulometric response based on exhaustive ion transfer may be hematocrit-dependent in whole blood tests.

In recent years, a wide variety of materials and chemicals such as redox polymers/molecules, capacitive carbon materials, nanostructured noble metals, metal-organic frameworks, intercalation compounds, and their combinations have been studied as the ion-to-electron transduction layer of solid-contact ISEs with the aim of improving the electrode-to-electrode consistency and other analytical performance characteristics.[11,12]

The deposited layer or suspension of redox-active solid contact materials such as conducting polymers may be further pre-polarized to unify standard potentials of multiple electrodes.[20-25] Although a few mV or less of standard deviations (SD) have been observed from the same batch of electrodes and occasionally from different batches, the reported variation is only for indicator electrodes as a shared reference electrode has been used in most studies. Since the EMF variation of reference electrodes is also a couple of mV or more,[11] full two-electrode potentiometric sensors are unlikely to have medically acceptable precision. Furthermore, it is important to consider that most of these small SDs have been obtained after soaking or subjecting the electrodes to electrochemical polarization in a standard solution for specific durations, typically ranging from 1 hour to 48 hours.[26] This lengthy and cumbersome conditioning process required right before conducting measurements is as impractical as the calibration process itself. The Buhmman group designed paper-based full potentiometric sensors that show an E° deviation of 3.2 mV in serum without conditioning, but "inner filling solutions" need to be added to complete the electrochemical cell at the point of use.[27] Recently, the pre-hydration of ion-selective membranes during the electrode preparation step has been investigated as a potential solution to mitigate the need for user-based electrode conditioning. [25] ISEs conditioned in a KCl solution and stored in a sealed package exhibit stable and reproducible response without prolonged on-site conditioning, but sensors were stored for only "at least 24 h" and bulky electrodes were used. Alternative methodologies aimed at reducing the conditioning times of ISEs focus on special analyte ions or rely on complex sensor arrangements that are not suitable for non-laboratory applications.[28,29] Therefore, it remains challenging to prepare simple, compact, and reliable ISE sensors that are free of calibration and conditioning at the point of use.

Herein, we report a completely new design of potentiometric sensors to enhance the reproducibility of EMF responses of ISEs. An ionic conductor such as an electrolyte solution is used to connect the sensing membrane and reference phase, which establishes an EMF baseline that corrects for sensor-to-sensor variations. When a sample is added, it induces a change in EMF, which is measured as the potentiometric response. This approach differs significantly from traditional potentiometry which relies on absolute EMF readings without a concept of baseline. Notably, there is a report on "self-calibrated" ion-selective electrodes,[30] but the principle of "self-calibration" is completely different and the sensor performance does not meet the requirements for decentralized electrolyte monitoring (12-h conditioning; large EMF errors).

EXPERIMENTAL SECTION

Reagents and Materials

Potassium ionophore I (valinomycin), potassium tetrakis [3,5-bis-(trifluoromethyl)phenyl] borate (KTFPB), 2-nitrophenyl octyl ether (NPOE), all of Selectophore™ grade, along with inorganic salts including potassium chloride (KCl), sodium chloride (NaCl), lithium chloride (LiCl), calcium chloride ($CaCl_2$), magnesium chloride ($MgCl_2$), lithium acetate (LiOAc), and sodium phosphate monobasic were purchased from MilliporeSigma. Low-molecular-weight polyethylene glycol diacrylate (PEGDA, n = approx. 9), amorphous fumed silica particles (surface treatment with dimethyldichlorosilane, ~325 mesh powder), sodium poly(4-styrenesulfonate) (NaPSS), EDOT 3,4-ethylenedioxythiophene (EDOT), lithium phenyl-2,4,6-trimethylbenzoylphosphinate, Ag wires (99.9%, 0.5 mm diameter), Au wires (99.9%, 0.5 mm diameter), Pt wires (99.9%, 0.3 mm diameter), and Polymicro Flexible Fused Silica Capillary Tubing (1068150023; ID: 100 μm, OD: 360 μm) were purchased from Fisher Scientific. HelixMark® Standard Silicone Tubing (60-011-07; ID: 1.58 mm, OD: 2.41 mm) was obtained from Freudenberg Medical. PTFE #30 AWG Thin Wall Tubing (06417-11; ID: 0.30 mm, OD: 0.76 mm) was purchased from Cole-Parmer.

Heparinized blood specimens were obtained from the Virginia Commonwealth University Medical Center. They are left-over blood from the Blood Gas Lab and deidentified before being collected by us. Heparinized human plasma was purchased from Innovative Research.

Preparation of K^+ ISEs

The indicator electrode comprises a PEDOT-coated Au wire inserted into a segment of plasticizer in a 1-cm long silicone tube. The cleaned Au wire is coated with PEDOT via galvanostatic polymerization in a three-electrode electrochemical cell consisting of a Ag/AgCl reference electrode and a Pt wire as the counter electrode.[31] The electrochemical cell contains a deaerated solution of 0.015 M EDOT and 0.1 M NaPSS. The electrosynthesis of PEDOT film on the ~1.5 cm end of a Au wire is performed at ~0.2 mA/cm^2 current density for 1428 s. The PEDOT-coated Au wire is air dried and stored in the dark overnight before use.

The K^+-selective oil is NPOE containing 1.0 wt% potassium ionophore I and 0.4 wt% KTFPB. The mixture is sonicated for 30 min to ensure complete dissolution of the sensing chemicals. Hydrophobic fumed silica nanoparticles are further mixed into the plasticizer solution at a ratio of 6.5% w/v to enhance its viscosity and mechanical strength.

Preparation of Reference Electrodes

The reference electrode comprises a Ag/AgCl wire coupled with a segment of PEGDA hydrogel containing inorganic salts. The Ag/AgCl wire is prepared via anodic electrodeposition of AgCl on a cleaned Ag wire in a 0.1 M NaCl solution. A 1-cm long silicone tube is filled with the low-molecular-weight PEGDA prepolymer mixed with 49.9 wt% aqueous solution and 0.1 wt% photoinitiator, lithium phenyl-2,4,6-trimethylbenzoylphosphinate. The aqueous solution contains 0.5 M LiOAc, 0.1 M LiCl, and 1 mM KCl unless otherwise specified. After the Ag/AgCl wire is inserted into the liquid mixture in the silicone tube, the tube is exposed to a planar UV light (Everbeam 365nm 100 W UV LED Black Light) for 30 s to obtain a photocured PEGDA-based reference electrode.

Preparation of Self-Calibrated Sensors

When the calibration phase is an aqueous solution, the solution is injected into a fused silica capillary tube or a PTFE tube. Two ends of the calibration tube are inserted into the plasticizer phase and the uncured PEGDA solution, respectively, with a depth of 2-3 mm on each side before photo-crosslinking is initiated for the reference electrode. When the calibration phase is an aqueous solution with PEGDA, it is first photocured in a calibration tube before the tube is inserted into the plasticizer phase and the reference solution. Then the reference solution is photocured to obtain a full self-calibrated sensor. The length of the calibration tube is ~ 1 cm for all self-calibrated sensors. All sensors are tested without any conditioning.

EMF Measurements

All EMF measurements are carried out at room temperature using an EMF-16 Precision Electrochemistry EMF Interface (Lawson Labs Inc.). For ion-selective sensors without the calibration bridge, the EMF is measured after a drop of aqueous sample is added into the gap between two silicone tubes. For ion-selective sensors with the calibration bridge, the EMF is measured before and after the addition of a drop of aqueous sample. A piece of Parafilm is always used underneath the sensor to prevent spreading of the aqueous solution. A Metrohm double-junction Ag/AgCl reference electrode is used as the reference electrode to test the performance of the PEGDA-based reference electrodes. The commercial and home-made reference electrodes are manually dipped into 2 mL of different solutions to test the EMF response of the PEGDA reference electrodes to salts. Liquid junction potential is calculated according to the stationary Nernst–Planck equation[32] using LJPcalc software (https://swharden.com/LJPcalc). Activity coefficients are calculated by the Debye–Hückel equation. For storage stability tests, self-calibrated sensors with the optimal reference and calibration composition are stored in a sealed two-layer plastic container with water in the bottom layer and sensors on the top layer. Response of fresh sensors and sensors after 3 and 6 weeks of storage is tested toward 10 mM KCl.

RESULTS AND DISCUSSION

Calibration Capability of the Ionic Conductor Integrated Between the Indicator and Reference Electrodes

PEDOT-based solid contact ISEs are used as an example to demonstrate the concept of self-calibrated potentiometric sensors because conducting polymer is one of the most commonly used solid contact materials. Potassium ionophore I and KTFPB are dissolved in NPOE via sonication without using any other solvents like tetrahydrofuran. The NPOE solution is further mixed with 6.5% w/v hydrophobic fumed silica particles as a thickening agent. The resulting NPOE-silica particle mixture is still easy to be transferred into the silicone tube via pipetting to create an ISE along with a PEDOT-coated Au wire, but the enhanced viscosity renders this "oil" phase mechanically more stable. The reference electrode is a Ag/AgCl wire inserted in a photo-crosslinked PEGDA hydrogel containing chloride ions. There is no microporous frit between the reference electrode and the sample, but the high rigidity of the solidified PEGDA hydrogel minimizes the mixing of the reference electrolyte and the sample (see below for optimization of the reference electrode). Figure 1A shows the setup of a tube type K^+ sensor. Figure 1B shows the EMF reading of n=5 sensors toward 1 mM KCl as the sample. Not surprisingly, the EMF reading of the full potentiometric sensor varies. The SD is 40.5 mV, which is consistent with the sensor-to-sensor variability of similar full sensors in a previous report.[9] The inconsistency is because the constituent conductors and interfaces such as the solid contact layer and the AgCl layer vary among multiple sensors even though they are identically fabricated.[11]

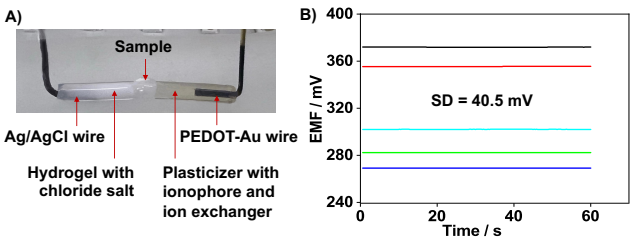

Figure 1. A: photo of a tube type potentiometric sensor consisting of a Ag/AgCl reference electrode and a ionophore-based solid-contact ion-selective electrode. Two tubes are silicone tubes to accommodate the hydrogel and the NPOE plasticizer phase for the reference and indicator electrode, respectively. The aqueous sample at a volume of 12 µL is added in between two silicone tubes. B: EMF readings of n=5 sensors to 10^{-3} M KCl.

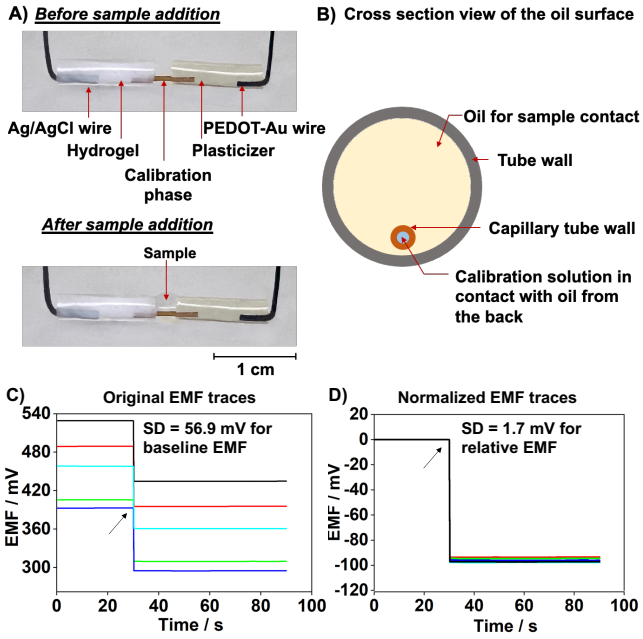

Figure 2. A: photos of a self-calibrated potentiometric sensor before and after the sample addition. B: the surface of the ion-selective oil that will be in contact with the sample. The fused capillary tube with the calibration solution is inserted into the oil. C: original EMF traces of n=5 self-calibrated sensors before and after adding 12 µL of 10^{-3} M KCl as the sample. D: EMF traces with all baseline values normalized to zero to aid in visualization of the consistency of the EMF changes. Black arrows in C and D indicate the addition of the sample.

Figure 2A shows the prototype self-calibrated sensor using the tube type design. The ion-selective oil and reference hydrogel are connected by a fused silica capillary tube with an ID of 0.10 mm and an OD of 0.36 mm. The tube has been filled with a solution containing the analyte ions (0.1 M KCl in this example). With this ionically conducting bridge, an EMF baseline can be first obtained in the absence of a sample, which is a unique feature of the proposed self-calibrated sensor as opposed to all previous potentiometric sensors. Then, a drop of aqueous sample is added to the space between two large silicone tubes to cover the exposed surface of the plasticizer phase in the indicator electrode and the hydrogel phase in the reference electrode. The EMF change upon sample addition is recorded and used for the quantification of K^+ in the sample. Figure 2C shows the baseline EMF and the EMF change after the addition of 12 µL of 10^{-3} M KCl as the sample. The baseline is further normalized to zero in Figure 2D to aid in visualization of the relative EMF. Although the original EMF baseline varies by tens of mV for n=5 sensors, the SD of the EMF change relative to the baseline (ΔEMF) is only 1.7 mV. All EMF variabilities from the electron conductors, solid contact layer, AgCl layer, and their interfaces are included in this baseline and compensated when ΔEMF is used for the response. The inconsistency in ΔEMF will only result from the variabilities in the interfaces between the two aqueous solutions (calibration solution and sample) and the two liquid-based electrode phases (plasticizer and

hydrogel). This inconsistency turns out to be much smaller probably because electric potential differences across interfaces between ionic conductors are well defined by the phase boundary potential model and the liquid junction potential theory.

Figure 3 shows the stepwise EMF response of the non-calibrated and self-calibrated sensors when the KCl concentration in the sample is increased from 10^{-4} to 10^{-1} M. The response slope of the self-calibrated sensors is 57.4 mV/decade, which is nearly identical to the slope of 57.8 mV/decade for sensors without the calibration tube, suggesting that the presence of an appropriate calibration bridge does not compromise the EMF response of the sample while serving for the calibration purpose.

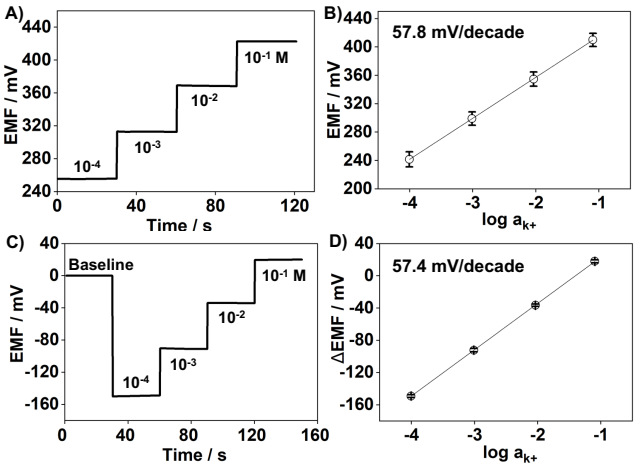

Figure 3. EMF traces and corresponding calibration curves of the potentiometric sensors without (A, B) and with (C, D) the calibration bridge. The concentrations denote KCl concentrations in the sample. Each sample is tested for 30 s and carefully removed before a new sample with a higher KCl concentration is added. N=3 sensors are tested for each type.

Optimization of the Calibration Bridge

In our sensor arrangement, one side of the ion-selective oil and the reference hydrogel are simultaneously exposed to two aqueous phases upon sample addition. To the best of our knowledge, similar designs have not been previously reported. An ISE or perhaps any indicator electrode of an electrochemical sensor is exposed directly to one external solution (usually a calibration solution or a sample) at one time. One immediate question and concern about the new design is that how the presence of a calibration phase affects the potentiometric response of the sample. Figure 4 shows the EMF baselines created by different calibration phases and the EMF changes after the addition of solutions containing 10^{-3}, 10^{-2}, and 10^{-1} M KCl. When the calibration tube has an ID of 0.30 mm and an OD of 0.76 mm and the calibration solution in this tube is 0.1 M KCl (Figure 4A), there are obvious upward EMF drifts after the addition of a KCl solution less concentrated than the calibration solution. In designing low-detection-limit ISEs based on classical planar polymeric membranes, the groups of Erno Pretsch and Eric Bakker studied the transmembrane ion flux from the inner filling solution with a higher primary ion concentration to the sample without primary ions.[33-35] Due to this chemical gradient-induced ion flux, the sample solution has an elevated primary ion concentration in the surface layer adjacent to the ion-selective membrane than the bulk. Since the ion-selective membrane senses the activity of primary ions in the interface zone of the aqueous sample, the EMF response appears greater than estimated based on the ion activity of the bulk sample solution. In our self-calibrated sensor configuration, the ion-selective oil is also exposed to two solutions with possibly different ion concentrations although both solutions are at the same side. Therefore, there should be a similar flux of the primary ions down the concentration gradient. In other words, the concentrated calibration solution contaminates the sample in our configuration similarly as the concentrated inner filling solution contaminates the sample in classical polymeric membrane ISEs. As EMF is proportional to the logarithm of the primary ion activity according to the Nernstian equation, the EMF increase caused by the contamination of a low-concentration solution is greater than the EMF decrease caused by the depletion of the concentrated solution. As a result, upward EMF drifts are observed in Figure 4A upon addition of a sample with a K^+ concentration low than the 0.1 M K^+ in the calibration tube.

Three strategies are examined to suppress the observed sample contamination and the resulting EMF drift. First, as shown in Figure 4B, 10^{-3} M instead of 10^{-1} M KCl as the calibration solution does not contaminate samples and therefore cannot induce significant EMF drifts. A slight upward drift for the 10^{-1} M KCl sample is likely caused by K^+ contamination in the opposite direction (from the sample to the calibration solution). As the electrolyte concentration in real samples especially body fluids usually have a narrow and known range, using a calibration solution containing a comparable concentration of the measuring ion should easily minimize contamination and EMF drifts. Second, when the contact area between the ion-selective

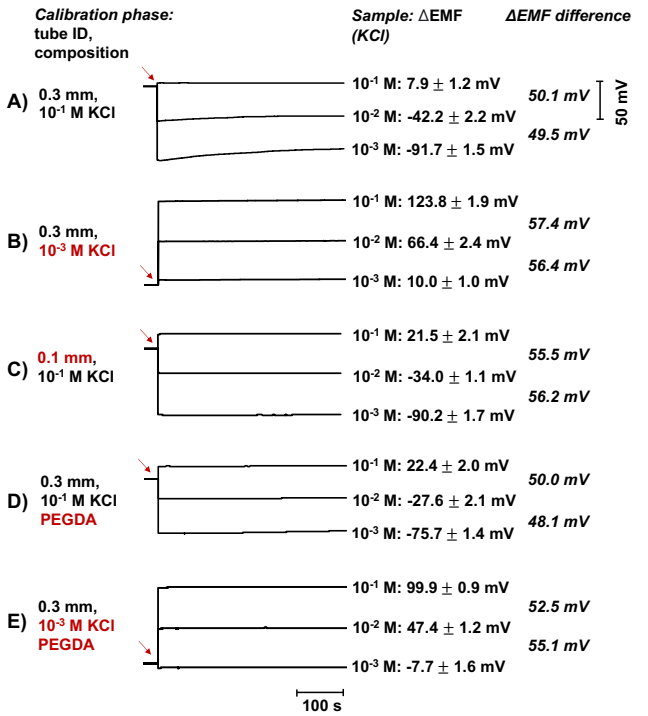

Figure 4. EMF traces of self-calibrated K^+-selective sensors before and after the addition of 12 µL of 10^{-3}, 10^{-2}, or 10^{-1} M KCl as the sample. Arrows indicate the sample addition. The EMF change relative to the baseline (ΔEMF after 400 s) for each KCl sample is labelled as average ± SD for n=3 sensors. The EMF difference between 10^{-3} and 10^{-2} M as well as 10^{-2} and 10^{-1} M KCl is labelled on the right to indicate the response slope.

oil and the calibration solution is much smaller than that between the oil and the sample, ion contamination caused by the calibration solution becomes less obvious. As can be seen from Figure 4C, EMF drifts are unnoticeable when the calibration tube ID is decreased to 0.1 mm although the calibration solution still has a high concentration of KCl (0.1 M). The oil-calibration solution contact area is only 0.4% of the oil-sample contact area (0.008 mm^2 vs. 1.889 mm^2) and the volume of the calibration solution is 150 times lower than the sample volume (0.08 µL vs. 12 µL). In contrast, the oil-calibration solution contact area is 0.071 mm^2 (4.6% of the oil-sample contact area) and the calibration solution volume is 0.76 µL (vs. 12 µL sample) in Figure 4A using a 0.3 mm ID calibration tube. A capillary tube with a tiny amount of salt solution is still able to complete the electrochemical cell as an ionic conductor to create a baseline prior to the sample addition, but it does not impair the sample response. Third, the EMF drift is reduced when the calibration phase is solidified by photo-crosslinked PEGDA (Figure 4D vs. Figure 4A while using the same concentration of KCl in the same 0.3 mm ID tube). Chemical diffusion in the PEGDA hydrogel is much lower than that in an aqueous solution,[36] which suppresses the overall ion flux from the concentrated calibration phase to the sample. If the KCl concentration in PEGDA is reduced to 10^{-3} M, the EMF drifts are eliminated as expected (Figure 4E). Although both liquid (Figure 4B, 4C) and hydrogel (Figure 4E) calibration phases enable drift-free EMF responses in these tube-type sensors, solidified hydrogel is more practical for other sensor configurations such as mass-producible planar sensors for long-term goals. Therefore, we will focus more on the photocured PEGDA calibration phase.

Interestingly, the use of a low concentration of primary ions (Figure 4B and 4E) or a small contact area between the calibration phase and the ion-selective oil (Figure 4C) also ensures the Nernstian response slope of the analyte ions in the sample. Classical response theories of ISEs such as Phase Boundary Potential model and the Nernst-Planck and Poisson equation were developed for well-defined, flat membranes with only one-dimensional ion gradients and electric potential profiles perpendicular to the membrane surface.[37,38] In the self-calibrated sensors, the presence of a common calibration phase with a fixed ion concentration may compromise the response slope as the concentration of the analyte ions in the sample change. The charge separation on the oil surface in contact with the calibration phase and the sample is governed by the primary ion concentration of the corresponding aqueous phase. The averaged charge density on the entire frontside surface of the ion-selective oil is determined by the total separated charge created by the calibration phase and the sample divided by the total interface area. When the calibration solution has a tiny contact area with the oil and/or the primary ion concentration is low, the charge separation and interfacial potential differences created by the calibration phase is small enough to be negligible. Therefore, the contribution of the calibration phase to the EMF reading in the presence of the sample is negligible, as evidenced by the close-to-Nernstian response slope in Figure 4B, 4C, and 4E. In summary, an appropriately formulated and sized calibration phase causes neither EMF drifts nor response slope reduction while providing a baseline for one-point calibration.

Optimization of the Reference Electrode

When the calibration phase and the reference phase have different compositions, chemical diffusion between two aqueous phases may happen during storage and impair the reliability of

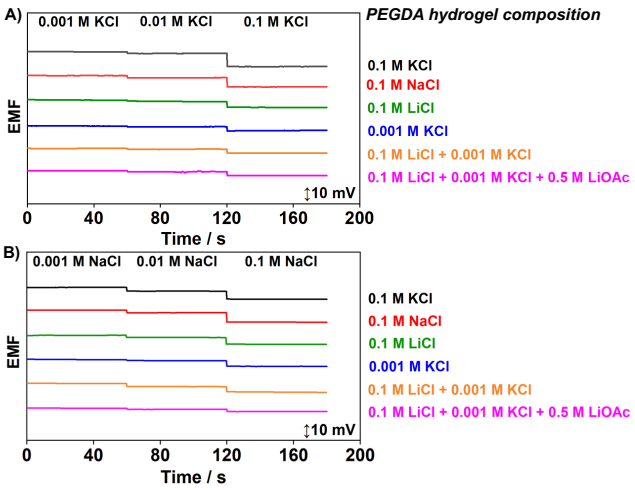

Figure 5. EMF response of different tube type reference electrodes to KCl (A) and NaCl (B) against a Metrohm double-junction Ag/AgCl reference electrode. The examined reference electrodes comprise Ag/AgCl wires coupled with PEGDA hydrogels containing different salts.

self-calibration. Therefore, it is best to employ the same composition for the calibration and reference phases. They are based on a PEGDA hydrogel instead of an aqueous solution because the hydrogel is preferred for the calibration phase and necessary to create a reference electrode that does not mix with the sample. The hydrogel should contain the analyte ion, K^+, for the calibration purpose, but the K^+ concentration should remain low to prevent contamination to the sample. Also, a high concentration of Cl^- is needed in the hydrogel to maintain a stable potential of the Ag/AgCl reference electrode. We systematically tested the performance of reference electrodes with different PEGDA-based hydrogel formulations to find one that meets the aforementioned requirements and exhibits most stable EMF as the sample composition changes. Figure 5 shows the EMF response of different reference electrodes to NaCl and KCl against a commercial double junction Ag/AgCl reference electrode. A high concentration of KCl or NaCl in the hydrogel makes the electrode more responsive to KCl or NaCl, respectively. The use of 0.1 M LiCl as the chloride salt reduces the EMF response towards both KCl and NaCl. Since the calibration phase needs a low concentration of K^+, a combination of 0.1 M LiCl and 1 mM KCl is an acceptable formulation. The addition of LiOAc, the commonly used equitransferent salt for reference electrodes, further reduces the EMF response especially toward NaCl. Therefore, the optimal formulation of our PEGDA-based reference phase has 1 mM KCl, 0.1 M LiCl, and 0.5 mM LiOAc. This Ag/AgCl reference electrode has an EMF response of –2.7 mV when NaCl is increased from 10^{-2} to 10^{-1} M. Since the commercial double-junction reference electrode using 1 M LiOAc as the bridge electrolyte has a calculated liquid junction potential of -2.9 and 0.3 mV for 10^{-2} and 10^{-1} M NaCl, respectively,[32] the observed EMF change (Figure 5B, magenta line) is largely due to the response of the commercial reference electrode instead of the optimal PEGDA reference electrode. Accordingly, this PEGDA reference electrode is unlikely to be sensitive to Na^+ fluctuations in most biological samples. Similarly, the junction potential for 10^{-3}, 10^{-2}, and 10^{-1} M KCl is -4.6, -3.2, and -1.4 mV, which accounts for a large portion of the observed KCl response in Figure 5A (magenta line) and thereby suggests low sensitivity of the optimal PEGD-based

reference electrode to KCl fluctuations in real samples. Moreover, the EMF of the PEGDA reference electrode remains constant when it is transferred from simple NaCl solutions in DI water to plasma and blood (Figure 6), indicating that there are no matrix effects from these complicated biological samples.

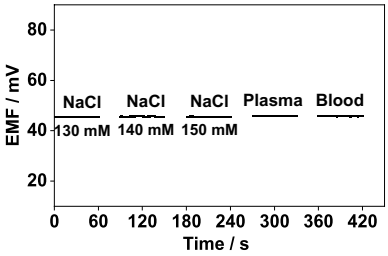

Figure 6. EMF response of the optimal PEGDA-based Ag/AgCl reference electrode in different aqueous solutions and body fluids against a commercial double junction Ag/AgCl reference electrode.

Traditional Ag/AgCl reference electrodes including those using hydrogels are separated from the sample via a pinhole, a capillary, a microporous junction, or a polymer layer to minimize mixing of the reference electrolyte and the sample.[39-41] In our design, the hydrogel in the silicone tube is in direct contact with the sample, but the mixing is suppressed by the crosslinked PEGDA network. Unlike traditional hydrogels such as agar, hydrogels formed from photo-crosslinking of low-molecular-weight PEGDA is rigid and the mesh size is only about 1-2 nm,[36] which is even smaller than the pore size of most junctions used in conventional reference electrodes.[42] While the aqueous solution trapped in the PEGDA network does not quickly mix with the aqueous sample, ions can diffuse across the interface, generating liquid junction potentials. The ion mobility in PEGDA hydrogel differs from that in simple aqueous solutions because a portion of water molecules are bound to polymers in hydrogels.[43] The ethylene glycol structure with electronegative O is also expected to bind to cations to reduce their mobility to different degrees. As a result, it is hard to calculate the liquid junction potential of each hydrogel formulation to explain the EMF response observed in Figure 5. Since the focus of this work is the novel self-calibration concept based on the ion-conducting bridge, the detailed working mechanism of the PEGDA reference electrode will be explored in future work.

Reproducibility, Blood Tests, and Storage Stability

The electrodes have been assumed to be single-use in optimizing the calibration phase and reference electrode. This is because home-use sensors for body fluids such as blood are supposed to be disposable and at-home electrolyte measurements using capillary blood are an urgent unmet need for the management of chronic diseases. When other sensing applications such as wearable, implantable, and in-field sensors for continuous ion monitoring are pursued in the future, more optimizations and assessments of the self-calibration methodology will be needed. Since blood K^+ concentrations always fall between 1 to 10 mM with a standard range of 3.5 to 5.5 mM, a calibration curve of the optimal self-calibrated K^+-selective sensor over 1 to 10 mM K^+ is constructed in Figure 7A. All standard solutions have an ionic strength of approximately 0.16 M and a pH of 7.4 to mimic the blood composition. The reproducibility of the relative EMF response of multiple sensors under these solution conditions is further confirmed for 1 mM and 10 mM KCl (n=10 sensors for each concentration). As can be seen from Figure 7B, the SD for 1 mM and 10 mM KCl is only 1.4 mV and 1.5 mV, respectively. According to the Nernstian equation, a 1.5 mV SD in EMF corresponds to a concentration SD of 0.3 mM for 5.0 mM K^+, which is below the acceptable K^+ measurement error of 0.5 mM according to the U.S. Code of Federal.[44]

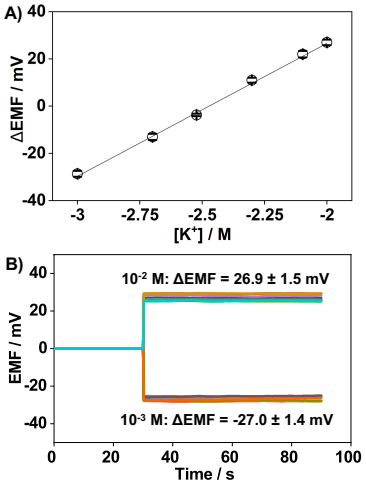

Figure 7. A) Calibration curve of the optimal self-calibrated K^+ sensor using the same PEGDA-based calibration and reference phases. Each sensor is used one time and the EMF change relative to the baseline after 1 min is calculated as the ΔEMF. All standard KCl solutions are prepared in 150 mM NaCl, 1 mM $CaCl_2$, 1 mM $MgCl_2$, and 2 mM phosphate buffer at pH 7.4. N=3 sensors are tested for each concentration. B) Reproducibility of the self-calibrated sensor in testing 10^{-3} and 10^{-2} M KCl, respectively. The baseline EMF is normalized to zero for all sensors and the relative EMF is shown as average ± SD for n=10 sensors.

Using the calibration curve in Figure 7A, the self-calibrated K^+ sensors are evaluated in 7 human blood specimens using an Abbott i-STAT blood gas analyzer as the reference technology. As shown in Table 1, the percent error ranges from 2.5 to 10.8%, indicating high accuracy of our sensors even though they are manually assembled. We noticed that the K^+ concentration determined by the self-calibrated sensor is always higher than that from the i-STAT analyzer. This positive deviation might be because of some systematic errors that are not identified such as errors of pipettes and balance used to prepare standard solutions. Furthermore, we conducted a preliminary study on the storage stability of the self-calibrated sensors. Since hydrogel in the reference and calibration phases may evaporate, sensors are stored in humidified air created in a sealed container with water on the bottom. The response of 10 mM KCl on

Table 1. K^+ concentration of seven human blood samples determined by the self-calibrated sensors and the Abbott i-STAT blood gas analyzer equipped with CHEM8+ cartridges.

Blood	1	2	3	4	5	6	7
This work (mM)	3.6	4.1	4.6	3.7	4.1	5.2	3.7
i-STAT (mM)	3.4	4.0	4.2	3.5	3.7	5.0	3.5
% Error	5.9	2.5	9.5	5.7	10.8	4.0	5.7

fresh sensors, sensors after 3-week storage, and sensors after 6-week storage is 27.1 ± 1.2 mV, 28.0 ± 0.6 mV, and 28.1 ± 1.1 mV, respectively. Each sensor is used for a single measurement and n=3 sensors are tested at each time point. This preliminary result is promising, and the storage stability may be further enhanced by utilizing professional packaging with more accurate humidity control.

CONCLUSIONS

A potentiometric sensor possesses an EMF baseline when the indicator and reference electrodes are linked through an ionic conductor. This integrated ionic conductor enables one-point calibration without compromising the response of the sample. Unlike traditional on-site calibration processes, this new calibration strategy does not require any fluid handling modules to deliver and clean calibration solutions. Design of planar ion sensors and multiplexed ion sensors with this self-calibration capability is underway in our laboratory. Other conductors such as conjugated polymers, carbon materials, and metals may also connect the indicator and reference electrodes to allow for the establishment of a baseline EMF. The storage and fabrication of these materials could be easier than aqueous solutions and hydrogels although their interfacial potentials may be harder to control. More electrochemical readout modes beyond open-circuit potential are also being explored on the ion-selective sensors with an integrated bridge in our laboratory.

AUTHOR INFORMATION

Corresponding Author

* Email: wangx11@vcu.edu

Present Address

†Department of Chemistry and Biochemistry, Florida Atlantic University, 777 Glades Road, Boca Raton, FL 33431

Author Contributions

The manuscript was written through contributions of all authors. All authors have given approval to the final version of the manuscript.

Notes

The authors declare no financial competing interest.

ACKNOWLEDGMENT

This work is financially supported by Virginia Commonwealth University (Startup Grant for X.W.) and Virginia Innovation Partnership Corporation (VIPC; CCF23-0065-HE).

REFERENCES

(1) Brandi, M. L.; Bilezikian, J. P.; Shoback, D.; Bouillon, R.; Clarke, B. L.; Thakker, R. V.; Khan, A. A.; Potts, J. T. Jr. Management of Hypoparathyroidism: Summary Statement and Guidelines. *J. Clin. Endocrinol. Metab.* **2016**, *101*, 2273-2283. DOI: 10.1210/jc.2015-3907

(2) Chang, A. R.; Sang, Y.; Leddy, J.; Yahya, T.; Kirchner, H. L.; Inker, L. A.; Matsushita, K.; Ballew, S. H.; Coresh, J.; Grams, M. E. Antihypertensive Medications and the Prevalence of Hyperkalemia in a Large Health System. *Hypertension* **2016**, *67*, 1181-1188. DOI: 10.1161/HYPERTENSIONAHA.116.07363

(3) Nilsson, E.; Gasparini, A.; Ärnlöv, J.; Xu, H.; Henriksson, K. M.; Coresh, J.; Grams, M. E.; Carrero, J. J. Incidence and Determinants of Hyperkalemia and Hypokalemia in a Large Healthcare System. *Int. J. Cardiol.* **2017**, *245*, 277-284. DOI: 10.1016/j.ijcard.2017.07.035

(4) Samantha, P.; Maxfield, F.; Elaine, P. Daily Sodium Monitoring and Fluid Intake Protocol: Preventing Recurrent Hospitalization in Adipsic Diabetes Insipidus. *J.E.S.* **2019**, *3,* 882–886. DOI: 10.1210/js.2018-00406

(5) Gao, F.; Liu, C.; Zhang, L.; Liu, T.; Wang, Z.; Song, Z.; Cai, H.; Fang, Z.; Chen, J., Wang, J.; Han, M.; Wang, J.; Lin, K.; Wang, R.; Li, M.; Mei, Q.; Ma, X.; Liang, S.; Guo, G.; Xue, N. Wearable and Flexible Electrochemical Sensors for Sweat Analysis: A Review. *Microsyst. Nanoeng.* ***2023****, 9*, 1. DOI: 10.1038/s41378-022-00443-6

(6) Heikenfeld, J.; Jajack, A.; Feldman, B.; Granger, S. W.; Gaitonde, S.; Begtrup, G.; Katchman, B.A. Accessing Analytes in Biofluids for Peripheral Biochemical Monitoring. *Nat. Biotechnol*. **2019**, *37*, 407–419. DOI: 10.1038/s41587-019-0040-3

(7) Zhao, J.; Guo, H.; Li, J.; Bandodkar, A. J.; Rogers, J. A. Body-Interfaced Chemical Sensors for Noninvasive Monitoring and Analysis of Biofluids. *Trends Chem*. **2019**, *1*, 559-571. DOI: 10.1016/j.trechm.2019.07.001

(8) Huang, X.; Zheng, S.; Liang, B.; He, M.; Wu, F.; Yang, J.; Chen, H.; Xie, X. 3D Assembled Microneedle Ion Sensor-Based Wearable System for the Transdermal Monitoring of Physiological Ion Fluctuations. *Microsyst. Nanoeng.* **2023**, *9*, 25. DOI: 10.1038/s41378-023-00497-0

(9) Gao, W.; Emaminejad, S.; Nyein, H.; Challa, S.; Chen, K.; Peck, A.; Fahad, H.M.; Ota, H.; Shiraki, H.; Kiriya, D.; Lien, D.; Brooks, G.A.; Davis, R.W.; Javey, A. Fully Integrated Wearable Sensor Arrays for Multiplexed *in Situ* Perspiration Analysis. *Nature* **2016***, 529*, 509–514. DOI: 10.1038/nature16521

(10) Parrilla, M.; Cuartero, M.; Crespo, G.A. Wearable Potentiometric Ion Sensors. *TrAC Trends Anal. Chem.* **2019**, *110*, 303-320. DOI: 10.1016/j.trac.2018.11.024

(11) Rousseau, C.R.; Bühlmann, P. Calibration-Free Potentiometric Sensing with Solid-Contact Ion-Selective Electrodes. *TrAC Trends Anal. Chem.* **2021**, *140*, 116277. DOI: 10.1016/j.trac.2021.116277

(12) Cheong, Y.H.; Ge, L.; Lisak, G. Highly Reproducible Solid Contact Ion Selective Electrodes: Emerging Opportunities for Potentiometry – A Review. *Anal. Chim. Acta* ***2021****, 1162, 338304*. DOI: 10.1016/j.aca.2021.338304

(13) Hu, J.; Stein, A.; Bühlmann, P. Rational Design of All-Solid-State Ion-Selective Electrodes and Reference Electrodes. *TrAC Trends Anal. Chem.* **2016**, *76*, 102-114. DOI: 10.1016/j.trac.2015.11.004

(14) Michalska, A.; Wojciechowski, M.; Bulska, E.; Maksymiuk, K. Experimental Study on Stability of Different Solid Contact Arrangements of Ion-Selective Electrodes. *Talanta* **2010**, *82*, 151-157. DOI: 10.1016/j.talanta.2010.04.012

(15) Grygolowicz, P.E.; Bakker, E. Background Current Elimination in Thin Layer Ion-Selective Membrane Coulometry. *Electrochem. Commun*. **2010**, *12*, 1195-1198. DOI: 10.1016/j.elecom.2010.06.017

(16) Shvarev, A.; Neel, B.; Bakker, E. Detection Limits of Thin Layer Coulometry with Ionophore Based Ion-Selective Membranes. *Anal. Chem.* **2012**, *84*, 8038-8044. DOI: 10.1021/ac301940n

(17) Vanamo, U.; Hupa, E.; Yrjänä, V.; Bobacka, J. New Signal Readout Principle for Solid Contact Ion-Selective Electrodes. *Anal. Chem.* **2016,** *88*, 4369-4374. DOI: 10.1021/acs.analchem.5b04800

(18) Han, T.; Mattinen, U., Bobacka, J. Improving the Sensitivity of Solid-Contact Ion-Selective Electrodes by Using Coulometric Signal Transduction. *ACS Sensors* **2019,** *4*, 900-906. DOI: 10.1021/acssensors.8b01649

(19) Tatsumi, S.; Omatsu, T.; Maeda, K.; Mousavi, M.P.S.; Whitesides, G, M.; Yoshida, Y. An All-Solid-State Thin-Layer Laminated Cell for Calibration-Free Coulometric Determination of K+. *Electrochim. Acta* **2022***, 408,* 139946. DOI: 10.1016/j.electacta.2022.139946

(20) He, N.; Papp, S.; Lindfors, T.; Höfler, L.; Latonen, R. M.; Gyurcsányi, R. E. Pre-Polarized Hydrophobic Conducting Polymer Solid-Contact Ion Selective Electrodes with Improved Potential Reproducibility. *Anal. Chem.* **2017**, *89*, 2598– 2605. DOI: 10.1021/acs.analchem.6b04885

(21) Vanamo, U.; Bobacka, J. Electrochemical Control of the Standard Potential of Solid-Contact Ion-Selective Electrodes Having a Conducting Polymer as Ion-to-Electron transducer. *Electrochim. Acta* **2014**, *122*, 316– 321. DOI: 10.1016/j.electacta.2013.10.134

(22) Vanamo, U.; Bobacka, J. Instrument-Free Control of the Standard Potential of Potentiometric Solid-Contact Ion-Selective Electrodes

by Short-Circuiting with a Conventional Reference Electrode. *Anal. Chem.* **2014**, *86*, 10540– 10545. DOI: 10.1021/ac501464s
(23) Papp, S.; Kozma, J.; Lindfors, T.; Gyurcsányi, R. E. Lipophilic Multi-walled Carbon Nanotube-based Solid Contact Potassium Ion-selective Electrodes with Reproducible Standard Potentials. A Comparative Study. *Electroanalysis* **2020**, *32*, 867– 873. DOI: 10.1002/elan.202000045
(24) Bahro, C.; Goswami, S.; Gernhart, S.; Koley, D. Calibration-Free Solid-State Ion-Selective Electrode Based on a Polarized PEDOT/PEDOT-S-Doped Copolymer as Back Contact. *Anal. Chem.* **2022,** *94*, 8302-8308. DOI: 10.1021/acs.analchem.2c00748
(25) Kozma, J.; Papp, S.; Gyurcsányi, R.E. TEMPO-Functionalized Carbon Nanotubes for Solid-Contact Ion-Selective Electrodes with Largely Improved Potential Reproducibility and Stability. *Anal. Chem.* **2022,** *94*, 8249-8257. DOI: 10.1021/acs.analchem.2c00395
(26) Conditioning times of different electrodes in Table 1 of Ref. 12: Ref. 91 (48h), 142 (overnight), 104 (overnight), 145 (no), 117 (1h), 64(1h), 113 (not specified), 62 (24h), 124 (24h), 126 (1 day), 112 (16h), 92 (>1h), 83 (>12h), 87 (not specified), 131 (overnight), 109 (1h), 84 (not specified), 63 (2 days), 66 (>6h).
(27) J, Hu.; A, Stein.; P, Bühlmann. A Disposable Planar Paper-Based Potentiometric Ion-Sensing Platform. *Angew. Chem. Int. Ed.* **2016**, *55*, 7544. DOI: 10.1002/ange.201603017
(28) Damala, P.; Zdrachek, E.; Forrest, T.; Bakker, E. Unconditioned Symmetric Solid Contact Electrodes for Potentiometric Sensing. *Anal. Chem.* **2022,** *94*, 11549-11556. DOI: 10.1021/acs.analchem.2c01728
(29) Rich, M.; Mendecki, L.; Mensah, S.T.; Blanco-Martinez, E.; Armas, S.; Calvo-Marzal, P.; Radu, A.; Chumbimuni-Torres, K.Y. Circumventing Traditional Conditioning Protocols in Polymer Membrane-Based Ion-Selective Electrodes. *Anal. Chem.* **2016,** *88*, 8404-8408. DOI: 10.1021/acs.analchem.6b01542
(30) Wang, F.; Liu, Y.; Zhang, M.; Zhang, F.; He, P. Home Detection Technique for Na^+ and K^+ in Urine Using a Self-Calibrated all-Solid-State Ion-Selective Electrode Array Based on Polystyrene−Au Ion-Sensing Nanocomposites. *Anal. Chem.* **2021**, *93,* 8318-8325. DOI: 10.1021/acs.analchem.1c01203
(31) Guzinski, M.; Jarvis, J.M.; Perez, F.; Pendley, B.D.; Lindner, E.; Marco, R.D.; Crespo, G.A.; Acres, R.G; Walker, R.; Bishop, J. PEDOT(PSS) as Solid Contact for Ion-Selective Electrodes: The Influence of the PEDOT(PSS) Film Thickness on the Equilibration Times. *Anal. Chem.* **2017,** *89*, 3508-3516. DOI: 10.1021/acs.analchem.6b04625
(32) Marino, M.; Misuri, L.; Brogioli, D. A New Open-Source Software for the Calculation of the Liquid Junction Potential Between Two Solutions According to the Stationary Nernst-Planck Equation. *arXiv preprint*. **2014**, *1403.3640*. DOI: 10.48550/arXiv.1403.3640
(33) Sokalski, T.; Ceresa, A.; Zwickl, T.; Pretsch, E. Large Improvement of the Lower Detection Limit of Ion-Selective Polymer Membrane Electrodes. *J. Am. Chem. Soc.* **1997**, *119*, 11347-11348. DOI: 10.1021/ja972932h
(34) Mathison, S.; Bakker, E. Effect of Transmembrane Electrolyte Diffusion on the Detection Limit of Carrier-Based Potentiometric Ion Sensors. *Anal Chem*. **1998**, *70*, 303-309. DOI: 10.1021/ac970690y
(35) Szigeti, Z.; Vigassy, T.; Bakker, E.; Pretsch, E.; Approaches to Improving the Lower Detection Limit of Polymeric Membrane Ion-Selective Electrodes. *Electroanalysis* **2006**, *18*, 1254-1265. DOI: 10.1002/elan.200603539
(36) Cruise, G. M.; Scharp, D. S.; Hubbell, J. A. Characterization of Permeability and Network Structure of Interfacially Photopolymerized Poly (Ethylene Glycol) Diacrylate Hydrogels. *Biomater.* **1998**, *19*, 1287-1294. DOI: 10.1016/S0142-9612(98)00025-8
(37) Bobacka, J.; Ivaska, A.; Lewenstam, A. Potentiometric Ion Sensors. *Chem. Rev.* **2008**, *108*, 329-351. DOI: 10.1021/cr068100w
(38) Bakker, E.; Bühlmann, P.; Pretsch, E. The Phase-Boundary Potential Model. *Talanta* **2004**, *63*, 3-20. DOI: 10.1016/j.talanta.2003.10.006
(39) Ciobanu, M.; Wilburn, J. P.; Buss, N. I.; Ditavong, P.; & Lowy, D. A. Miniaturized Reference Electrodes Based on Ag/AgiX Internal Reference Elements. I. Manufacturing and Performance. *Electroanalysis* **2002**, *14*, 989-997. DOI: 10.1002/1521-4109(200208)14:14<989::AID-ELAN989>3.0.CO;2-6
(40) Ha, J.; Martin, S. M.; Jeon, Y.; Yoon, I. J.; Brown, R. B.; Nam, H.; Cha, G. S. A Polymeric Junction Membrane for Solid-State Reference Electrodes. *Anal. Chim. Acta* **2005**, *549*, 59-66. DOI: 10.1016/j.aca.2005.06.011
(41) Liao, W. Y.; Chou, T. C. Fabrication of A Planar Form Screen-Printed Solid Electrolyte Modified Ag/AgCl Reference Electrode for Application in a Potentiometric Biosensor. *Anal Chem.* **2006**, *78*, 4219-4223. DOI: 10.1021/ac051562+
(42) Anderson, E. L.; Troudt, B. K.; Bühlmann, P. Critical Comparison of Reference Electrodes with Salt Bridges Contained in Nanoporous Glass with 5, 20, 50, and 100 nm Diameter Pores. *Anal. Sci.* **2020**, *36*, 187-191. DOI: 10.2116/analsci.19P235
(43) Gun'ko, V. M.; Savina, I. N.; Mikhalovsky, S. V. Properties of Water Bound in Hydrogels. *Gels* **2017**, *3,* 37. DOI: 10.3390/gels3040037
(44) Laboratory Requirements, Code of Federal Regulations, Section 493.931, Title, 42, 2003

Table of Contents